Colloids and Surfaces A 606 (2020) 125478

Contents lists available at ScienceDirect

Colloids and Surfaces A

journal homepage: www.elsevier.com/locate/colsurfa

Viscoelastic properties of interfacial lignosulfonate films and the effect of added electrolytes

Jost Ruwoldt*, Sébastien Simon, Gisle Øye

Ugelstad Laboratory, Department of Chemical Engineering, Norwegian University of Science and Technology (NTNU), Trondheim, Norway

GRAPHICAL ABSTRACT

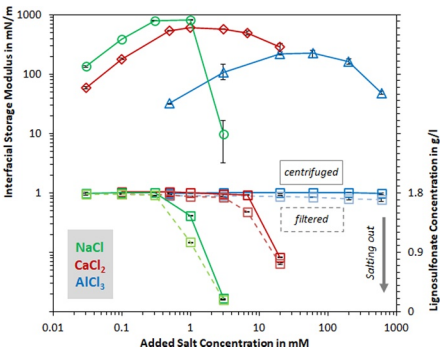

ARTICLE INFO

Keywords:
Lignosulfonate
Dilatational interfacial rheology
Interfacial shear rheology
Film stability
Emulsion stabilization
Ward and Todai

ABSTRACT

New evidence is presented, which confirmed interfacial gelling of lignosulfonates in presence of di- and trivalent cations. In this article, the viscoelastic properties of lignosulfonate films at the water-xylene interface were studied by dilatational interfacial rheology and interfacial shear rheology. Both techniques showed that increasing lignosulfonate concentration would first increase and then decrease the interfacial modulus. The same trend was observed for increasing salinity. The maximum interfacial modulus corresponded with lignosulfonate aggregation or precipitation and accounted for the best emulsion stability. The film strength increased progressively with the cation charge number. It was argued that multivalent cations provided intermolecular bridging between lignosulfonate molecules, which increased film strength and led to gelling. The decrease of interfacial film strength at high salinity was explained by two mechanisms: (1) For sodium cations, the polyelectrolyte contraction at high ionic strength yielded screening of the functional groups, which are deemed responsible for attractive interactions between lignosulfonate molecules or aggregates. (2) For calcium and aluminum cations, precipitation would reduce the effective bulk concentration, yielding a lower surface coverage. Modelling of the interfacial properties was conducted in addition, which showed that lignosulfonate adsorption was not diffusion-controlled and that lignosulfonate aggregation was affecting the adsorption process. In conclusion, our results revealed a more detailed picture of the mechanisms, which govern the interfacial behavior and properties of lignosulfonates.

* Corresponding author.
E-mail address: jostru.chemeng@gmail.com (J. Ruwoldt).

https://doi.org/10.1016/j.colsurfa.2020.125478
Received 23 June 2020; Received in revised form 17 August 2020; Accepted 18 August 2020
Available online 05 September 2020

1. Introduction

Lignosulfonate is a versatile dispersant that can be used to stabilize dispersions, emulsions and suspoemulsions [1]. It is hence found in applications such as dye dispersants, water reducers of cement, animal feed additives, wastewater treatment, coal-water slurry dispersants and petroleum production [2]. Lignosulfonates are produced by sulfite pulping of wood and are therefore considered a green and renewable alternative to many synthetic chemicals.

Sulfite pulping of wood has historically been used to soften the lignin and render it more hydrophilic, with the goal of liberating the cellulosic fibers for paper production [3]. During this process, the lignin polymer is broken down and sulfonate groups are introduced onto the polyaromatic backbone of the lignin fragments [4]. The resulting product, lignosulfonate, hence comprises both hydrophobic and hydrophilic moieties. Good water solubility is accounted for by the anionic groups, which are sulfonate, carboxyl, and at high pH phenolic groups [5].

The chemical makeup of lignosulfonates is mostly derived from the precursor lignin. Lignin is a complex aromatic heteropolymer that is synthesized from the monolignols phydroxyphenyl (H unit), guaiacyl (G unit), and syringyl (S unit) phenylpropanoid [6]. While coniferous lignin (softwood origin) is composed of mainly G units, lignin from broadleaved trees (hardwood origin) contains a mix of G and S units [7]. The ratio of G, S and H units can affect both the reactivity of lignin, but also the composition and properties of the produced lignosulfonates [4]. For example, hardwood was reported to yield lower molecular weight lignosulfonates than softwood [8]. Softwood lignosulfonates were reported to exhibit better salt tolerance and to possess a Hansen solubility parameter closer to water [9,10].

In aqueous solutions, lignosulfonates are said to assume a flat spheroid shape, which may self-associate on the long edges to form aggregates [11,12]. Aggregation is the result of hydrophobic interaction, as the hydrophobic backbones are bundled together in the aggregate center [13]. The aggregate surface is largely covered by ionizable functional groups, such as sulfonate and a few carboxylic and phenolic groups. Lignosulfonate aggregation can be caused by increasing lignosulfonate concentration, increasing salinity, or the addition of alcohol [12,14]. This was explained by a decrease of surface charge, which further facilitated interparticle association [12]. It has also been reported that increasing temperature can induce lignosulfonate aggregation [15]. Increasing the pH from 2 to 10 yielded increase in the dimensions of both dissolved and aggregated lignosulfonate, as this would increase the degree of ionization of functional groups and hence promote structural unfolding [13,16]. Under standard conditions the sulfonate groups remain mostly dissociated, whereas the carboxylic groups dissociate at around pH 3–4 and the phenolic groups at around pH 9–11 [13,17]. Precipitation and flocculation can be caused by adding salt to a lignosulfonate solution. This saltingout tendency followed the Hofmeister series with the exception of a few ions [5].

Lignosulfonate can adsorb readily from solution on surfaces and interfaces. The adsorption on solid surfaces was reported to follow the Langmuir isotherm [18–20]. Surface activity of lignin products can be studied by measuring surface tension [19,21]. This approach was for example used to elucidate interactions of lignosulfonates with straight-chain alcohols, anionic or cationic surfactants [22–24]. Mixing lignosulfonates and petroleum sulfonate yielded the low interfacial tension needed for enhanced oil recovery [25]. Some authors used surface tension measurements to determine the critical aggregation concentration (CAC) of lignosulfonates [23], however, large discrepancies exist when comparing e.g. with fluorescence spectroscopy [13,26]. Langmuir trough system had been used to record lignosulfonate compression isotherms [27]. The obtained multilayers were readily compressible, where the film stability depended largely on the type and amount of the added electrolyte. Increasing the ionic strength of lignosulfonate solutions, e.g. by NaCl addition, led to a logarithmic decrease in surface tension [22,28]. Selfassembly of lignosulfonate and cationic polymer was investigated, based on which the authors concluded that the adsorption process was not mainly driven by electrostatic interaction, but by cation-π interaction and hydrophobic interaction [29,30]. Complexation of lignosulfonate and watersoluble cationic surfactant furthermore yielded a material, which was more hydrophobic than the precursors [31].

The ability of lignosulfonates to stabilize oil in water emulsions has been demonstrated and was shown to also affect emulsion rheology and creaming rates [32,33]. A combination of electrostatic repulsion, stearic hindrance, particle stabilization, and the formation of a semi-rigid interface layer were stated as emulsion stabilization mechanisms [14,34]. It has long been established that droplet coalescence is affected by the stability of interfacial layers, which can be formed by adsorbing species such as surfactants or polymers [35]. Over the years, various experimental techniques and setups have been developed to study the rheology of such layers. These techniques can exploit measuring principles such as rotational shear, oscillation of droplet volume, oscillation of barrier position and capillary waves [36]. Oscillation of droplet volume will further be referred to as dilatational interfacial rheology in this article. This technique has been applied to measure both simple and complex interfacial layers, which were formed by materials such as surfactants, proteins, polymers or micro and nano-sized particles [37]. Application areas for rotational shear rheology include emulsifiers and proteins for food industry, crude oil indigenous components with relevance to petroleum production, and surfactant science [38–41]. Overall, the knowledge of interfacial rheology is key to engineering processes that deal with emulsions, micelles, foams or dispersions [42].

Lignosulfonates are known oil-in-water emulsion stabilizers, yet the research on lignosulfonate behavior at liquid-liquid interfaces is very limited. Recent developments have yielded lignosulfonate products, which are more hydrophobic and hence possess improved efficiency as emulsion stabilizers. The objective of this article is therefore to extend interfacial rheology to investigate lignosulfonates. Both interfacial dilatational rheology and interfacial shear rheology were applied and correlated. The key parameters studied were lignosulfonate concentration and salinity. Lignosulfonate salting out and effect on emulsion stability were explored for comparison and to provide a more complete picture. At last, modelling of the experimental data was done, and physicochemical mechanisms were proposed to explain the observed trends.

2. Experimental section

2.1. Materials

A commercial sodium lignosulfonate was provided by Boregaard Lignotech. This lignosulfonate was selected, as it exhibited the highest interfacial moduli of all tested samples. All water was purified with a Millipore water purification system (resistivity 18.2 MΩ). The organic phase used in this study is xylene isomer blend (≥97 %, HPLC-grade) and was purchased from VWR, Norway. Xylene was selected, as aromatic solvents yielded higher interfacial moduli than alkane-based solvents for the studied lignosulfonate, which provided the best sensitivity for interfacial shear rheology. Salts were obtained as chloride (≥99.5 %), calcium chloride dihydrate (≥99 %) and aluminum chloride hexahydrate (≥97 %) from Sigmaaldrich, Norway.

2.2. Sample and experiment preparation

Solutions were prepared by weighing stock solutions of lignosulfonate and salt into volumetric flasks. At first, the lignosulfonate was added, then followed by water. The stock solution of salt was always added last and only after initial lignosulfonate dilution. This was done to prevent irreversible agglomeration of the lignosulfonate. The

solutions were sonicated for 10 min and aged overnight at ambient conditions before use. No influence of aging time beyond overnight storage was found concerning the interfacial properties. A more elaborate procedure was used for solution preparation of salt tolerance experiments, which involved temperature-controlled equilibration at 25 °C for exactly 18 h before further sample processing.

The bulk densities and viscosities were required as input parameters for interfacial tension or interfacial rheology measurements and to determine the lignosulfonate concentration from UV spectrometry. Density measurements were conducted on a DMA 5000 M density/concentration meter and viscosity measurements on a Physica MCR 301 rotational shear rheometer, which were both manufactured by Anton Paar, Austria. For viscosity measurements, the rheometer was equipped with CC27/T200 bob-cup geometry.

2.3. Pendant drop video tensiometer

Pendant drop experiments were conducted using a PAT 1 m video tensiometer from SINTERFACE Technologies, Germany. During experimentation, the pendant aqueous droplet is suspended from a cylindrical tube and submerged in the oil phase, xylenes. The interfacial tension is measured by recording the silhouette of the pendant droplet via a CCD camera. The digital images are analyzed in real-time and fitted to the Young-Laplace equation with an accuracy of 0.1 mN/m. The Young-Laplace equation relates the curvature of the liquid drop to the surface or interfacial tension, which is then calculated via an iterative procedure in the software. This technique is also known as axis symmetric drop shape analysis (ADSA) and requires only the phase densities as input parameters. The droplet volume is controlled by the software via constant feedback.

A new droplet was created at each experiment start. Interfacial tension was recorded in 1 s intervals. Droplet volume oscillations were initiated after 5 h equilibration time. The equilibration time for interfacial rheology measurements is further discussed in section 3.1. Oscillations were done at frequencies of 0.01, 0.0125, 0.0167, 0.025 and 0.05 Hz with four repetitions each and an amplitude of 7.5 %, which corresponded to 30 ± 2.25 µl droplet volume in most experiments. For samples with low interfacial tension (~12 mN/m and lower), the droplet volume was decreased to 25 or 20 mL, as droplet loss could otherwise occur. All experiments were conducted in duplicates and reproducibility was generally within 1 mN/m.

The principle behind dilatational interfacial rheology as follows: Upon the appearance of oscillating changes in the surface area, the surface tension proceeds with a lag phase, which is dependent on the viscoelastic properties of the interfacial layer [36]. If the surface area $A(t)$ is oscillating with a low amplitude at frequency ω, then the change in surface tension $\sigma(t)$ is linear, as expressed by Eqs. (1) and (2).

$$A(t) = A_{surf,0} + A_0 \sin(\omega t) \tag{1}$$

$$\sigma(t) = \sigma_{surf,0} + \sigma_0 \sin(\omega t + \delta) \tag{2}$$

Here, A_0 and σ_0 are the respective surface area and surface tension amplitudes, $A_{surf,0}$ and $\sigma_{surf,0}$ are the surface area and surface tension prior to oscillation, and δ is the phase angle. The complex 2D elastic modulus E^* is further determined via Eq. (3), where E' is the real component characterizing the elastic properties of the interfacial layer (apparent elastic dilatational modulus) and E'' is the imaginary component characterizing the viscous properties (apparent viscous dilatational modulus).

$$E^*(\omega) = E'(\omega) + iE''(\omega) = \frac{d\sigma(t)}{d\ln A(t)} \tag{3}$$

The concept of dilatational elastic modulus E^* is in analogy to the complex elastic modulus G^* in shear rheology. Moreover, the contributions of extra mechanical stresses on the interface must be negligible for the YoungLaplace equation to remain valid [43]. This requirement is fulfilled in case of the viscoelastic interface layers formed by sodium lignosulfonate, however, adding multivalent cations could render the interfacial films partially incompressible. Such partial incompressibility was observed, for example, as a wrinkling of the droplet surface upon volume contraction as shown in Fig. 1. In addition, the measurements were no longer within the linear viscoelastic range for such samples. Dilatational interfacial rheology was therefore applied to study lignosulfonate and NaCl dosing only.

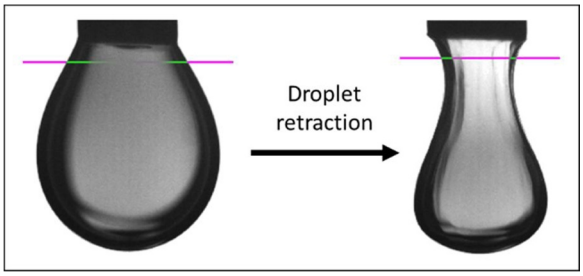

Fig. 1. Images of droplet retraction in pendant drop video-tensiometry. An incompressible interface layer formed by lignosulfonate in presence of calcium ions is visible as wrinkling of the droplet surface.

2.4. Rotational shear rheometer

Interfacial shear rheology was conducted on a Physica MCR 301 rotational shear rheometer from Anton Paar, Austria. The rheometer was equipped with a biconical bob geometry that had a cone radius of 34.14 mm, cone angle of 5° and cone height of 2.235 mm. The geometry was suspended into the temperature-controlled cup with an inner radius of 40.00 mm and height of 45.00 mm. After each experiment, the interfacial modulus was numerically computed from the measured data in the Rheoplus software, which also corrected contributions due to the flowfield of the bulk liquids. A method description and discussion of the advantages and shortcomings of this technique has been published by Erni et al. [44].

During experiment preparation, the rheometer cup was loaded with 110 mL of aqueous phase (bottom phase) containing the lignosulfonate and added salt. The bi-conical bob was then moved closely above the aqueous phase surface. While being lowered at a rate of 10 µm/s, the exact position of the cone tip touching the surface was determined via a force transducer. The outer rim of the bicone was positioned at the interface by subtracting the cone height (2.235 mm) from the tip-surface position. In the next step, 105 mL of xylenes (top phase) were carefully added using a pipette to minimize disturbances. Rheology measurements were started immediately after adding the top phase.

The experimental protocol consisted of an equilibration period, followed by a frequency and a strain sweep. During the equilibration period, continuous oscillations at 1 Hz and 0.2 % strain were imposed. This strain was within the linearviscoelastic range for all experiments. The frequency sweep was conducted logarithmically increasing from 0.01–10 Hz at 0.2 % strain. The strain sweep increased logarithmically from 0.0001–100 % at 1 Hz. Experiments were conducted at 25 °C. After each experiment, the viscous force-contributions of the bulk media were numerically subtracted from the measured data in the RheoPlus software.

During interfacial shear rheology, an azimuthal shear deformation is applied to the interface while preserving constant interface area. The measuring principle is based on recording the shear stress $\tau(t)$ in response to a sinusoidal deformation $\gamma(t)$ at angular frequency ω [40]. As stated in Eqs. (4) and (5), this also relates the strain and stress amplitude γ_0 and τ_0, respectively, with the phase angle δ.

$$\gamma = \gamma_0 \sin(\omega t) \tag{4}$$

$$\tau = \tau_0 \sin(\omega t + \delta) \tag{5}$$

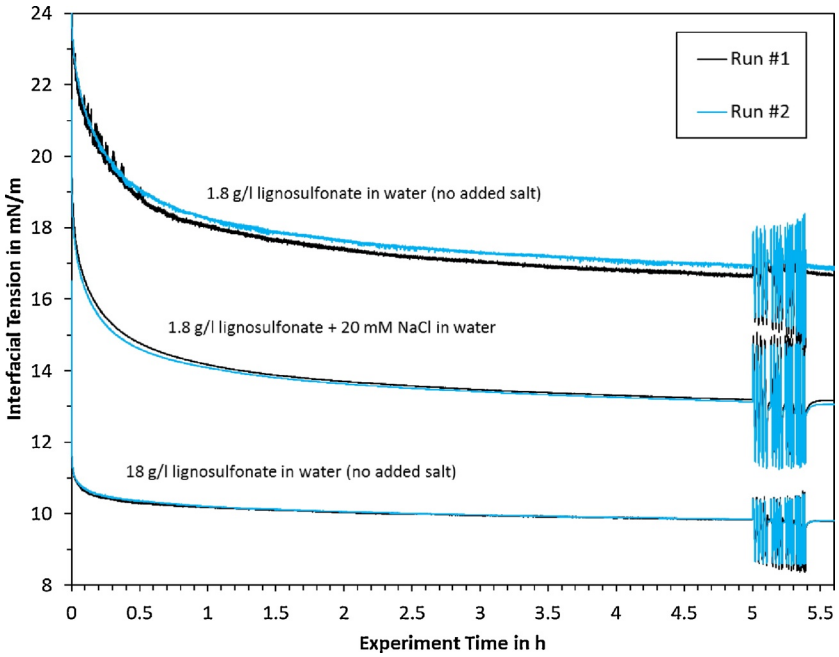

Fig. 2. Progression of interfacial tension with time during pendant drop experiments.

The complex shear modulus G^* is further composed of the sum of storage modulus G' (in-phase response) and loss modulus G'' (out-of-phase response), which can be individually computed via Eqs. (6) and (7).

$$G' = \frac{\tau_0}{\gamma_0}\cos(\delta) \tag{6}$$

$$G'' = \frac{\tau_0}{\gamma_0}\sin(\delta) \tag{7}$$

Interfacial shear rheology differs from dilatational interfacial rheology, which periodically increases and decreases the interface area. As the interface area remains constant, interfacial shear rheology returns only the pure rheological response of the interface, which lacks the diffusional contribution.

2.5. Lignosulfonate salting out and salt tolerance

A mechanical separation procedure was applied to study the dispersion state of lignosulfonates, which was based on our previous efforts to measure lignosulfonate salt tolerance. Sample solutions were prepared and after 18 h of equilibration period, 40 mL of lignosulfonate and salt solution/dispersion were filled into a vial. The vial was sealed and centrifuged in an Eppendorf 5810 centrifuge for 5 min at 8000 rpm. Afterwards, the top 30 mL of supernatant were decanted and collected for UV analysis. Part of the collected supernatant was also filtered through 0.2 µm polypropylene syringe filter, collected and analyzed.

Quantification of lignosulfonate concentration was done on a Shimadzu UV-2401PC UV/vis spectrometer. Both the unfiltered and filtered sample were diluted by a factor of 50–100 in water before analysis. The absorbance at 280 nm was used for measuring the concentration of the dilute lignosulfonate solution. Calibration was done with known dilutions of this sample. The absorbance was linearly proportional to the lignosulfonate concentration within the established limits, which also showed that lignosulfonate agglomeration did not occur in the analyte.

In preliminary experiments it was established that above a certain salt concentration, lignosulfonate would form flocculates that are quickly removed by centrifugation. Prolonged centrifugation did not substantially change the amount of sediment. Filtration however could further reduce discoloration and increase transparency of the solution. The presented separation procedure was therefore developed to study the lignosulfonate dispersion state. A concentration decrease after centrifugation was attributed to lignosulfonate precipitation, as this removed the larger flocculates. A concentration decrease after filtration was associated with agglomerate growth, since some lignosulfonate agglomerates had become as large as that they could be retained by the filter.

2.6. Emulsion stability

Lignosulfonate effect on emulsion stability was also tested in analogy to a previously published procedure [45]. Firstly, the organic phase (xylene) was emulsified in the aqueous phase by mixing at 18 000 rpm with an Ultra Turrax T 25 homogenizer fitted with an 18 mm head from IKAWerke GmbH & Co. KG, Germany. The emulsions were prepared in centrifugation vials, sealed, stored overnight, and processed the next day. Processing started with centrifugation at 10 000 rpm for 10 min in an Eppendorf 5810 centrifuge. Afterwards, the free oil layer on top of the emulsion was carefully removed, collected, and weighed. The weight of recovered oil was divided by the initial amount of xylene, which yielded the oil recovered percentage. Two to three measurements were made per sample and reproducibility was within ± 5 wt.% or better.

3. Results and discussion

3.1. Interfacial tension and dilatational interfacial rheology

The progression of interfacial tension with time is exemplarily plotted for three samples in Fig. 2. Right after the experiment start, the interfacial tension decreased rapidly. As experiment time progressed, the slope of this decrease became lower. At 5 h of experiment time, the interfacial tension is varied in an oscillating manner, which is due to the start of dilatational interfacial rheology measurements. As can also be seen, the duplicate runs are in close agreement for each sample.

Upon the start of droplet oscillations, the interfacial tension should ideally have reached a constant value. Test runs over longer time periods had shown that even after 3 d of equilibration time, the interfacial tension was still subject to change. Such behavior is likely rooted in the

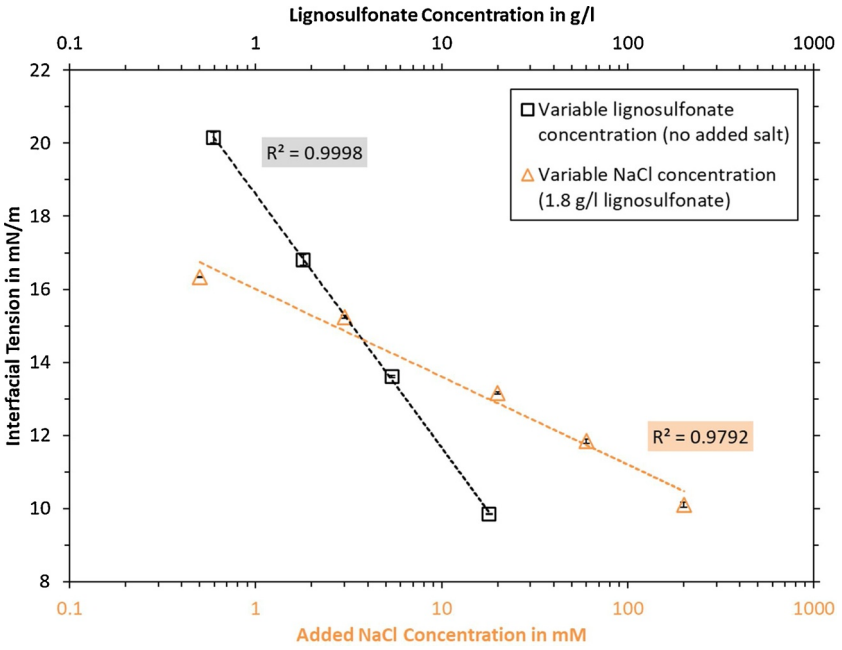

Fig. 3. Effect of lignosulfonate or NaCl concentration on interfacial tension as measured by pendant drop technique. The dotted line represents a logarithmic regression function.

makeup and polydispersity of the lignosulfonate sample. It is proposed that the lignosulfonate molecules undergo diffusion exchanged at the interface. In addition, the molecules could be subject to rearrangement, both with respect to each other and with respect to the water-oil interface. Analogous mechanisms have been described e.g. to explain the behavior of adsorbed petroleum asphaltenes [46,47].

As the exact equilibration time was difficult to determine, a specific time interval was used instead. This approach provided consistency and had been used by other authors for similar experiments [27,40,43,48]. A duration of 5 h was chosen for practical reasons and because most of the tested samples showed a plateauing of the interfacial modulus at this equilibration time.

The interfacial tension measured is plotted in Fig. 3. As can be seen, it is decreasing logarithmically with respect to lignosulfonate or NaCl concentration. Such a behavior is in correlation with results interfacial or surface tension published previously [22,45,49]. Scattering was more pronounced for NaCl dosing experiments, but the data is still following the regression line.

The interfacial storage and loss moduli are plotted in Fig. 4 for varied lignosulfonate concentration. Increasing the lignosulfonate concentration from 0.6–18 g/l would first increase and then decrease the interfacial storage or loss modulus with a local maximum at 5.4 g/l or 1.08 g/l, respectively. A similar dependency of interfacial moduli on component concentration has been observed for interface layers formed by e.g. petroleum indigenous components [50] or nonionic surfactant [51]. In addition, the storage moduli are consistently larger at higher frequency than at lower frequency.

The evolution of interfacial modulus in dependence of added NaCl concentration is plotted in Fig. 5. Similar as to Fig. 4, an increase in NaCl concentration yielded first an increase and then a decrease in interfacial modulus with a local maximum. The maximum storage modulus after NaCl addition is higher than for pure lignosulfonate, but overall values are on the same order of magnitude. One notable difference between Figs. 4 and 5 is the variation with frequency. In Fig. 5, the storage modulus is greater at higher frequencies and low NaCl concentrations, but at NaCl concentrations of 60 mM and higher there are almost identical storage moduli at the different frequencies. Such behavior is not typical for a diffusion-controlled process, suggesting that at high NaCl concentrations the interface behavior is governed by other mechanisms such as a viscoelastic response.

3.2. Interfacial shear rheology

The buildup of an interfacial layer in shear rheology followed similar kinetics as the interfacial tension in pendant drop experiments. The equilibration time was set to 5 h to ensure good comparison with dilatational interfacial rheology. The storage and loss modulus at 5 h after experiment start are plotted in Fig. 6. After the equilibration period, a frequency sweep and subsequent strain sweep were conducted, which are plotted in Figs. 7 and 8.

The development of storage modulus with respect to lignosulfonate or NaCl concentration in Fig. 6 is coherent with the trends discussed in section 3.1, that is, both storage and loss modulus exhibit a maximum at intermediate concentration. There are, however, differences between the results obtained from dilatational interfacial rheology and interfacial shear rheology. Firstly, in shear rheology the storage and loss moduli are more similar, both in terms of the qualitative progression and in terms of the numerical values. At low lignosulfonate concentrations (1.08 g/l and less) the loss modulus was higher than the storage modulus. Moreover, the storage modulus measured by interfacial shear rheology is about five times higher compared to dilatational interfacial rheology. Such a difference is not surprising, because the measuring principle is different. In interfacial shear rheology, the mechanical response is purely due to the viscoelastic property of the interface layer, which excludes the adsorption and desorption effects encountered in dilatation interfacial rheology. Such effects would result in a reduction of measured storage modulus, which is in line with the observations. In addition, the applied frequencies are different by more than one magnitude, that is, 1 Hz in interfacial shear rheology and 0.01 – 0.05 Hz in dilatational interfacial rheology. On the other hand, it is interesting to note that the two techniques measured the same qualitative trend with respect to the interfacial storage modulus. In both cases, the maximum storage modulus was measured at 5.4 g/l lignosulfonate in water without added salt. In case of NaCl dosing, the maximum was recorded at 20 mM for dilatational interfacial rheology and 60 mM for interfacial shear rheology.

One of the goals of this study was to investigate the effect of different cations. The type of anion was kept the same for better

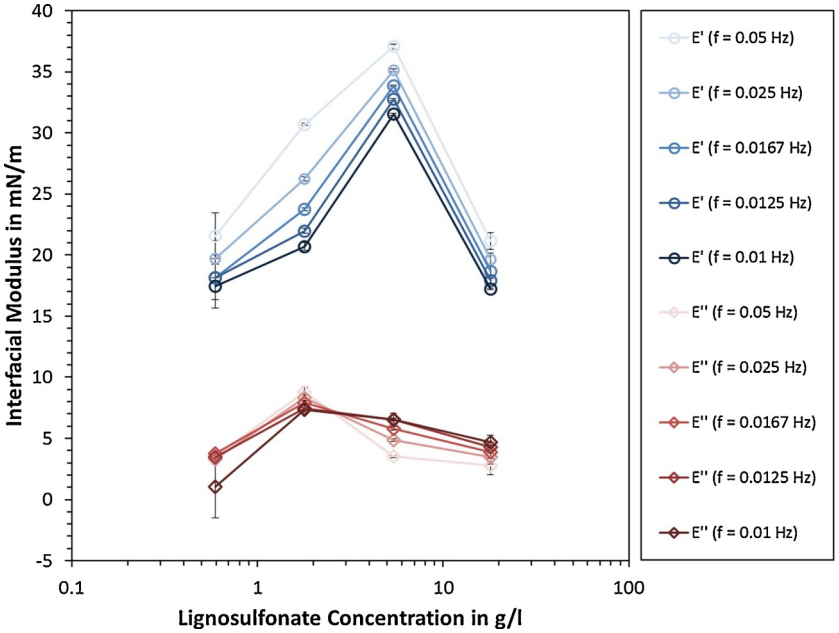

Fig. 4. Interfacial moduli in dependence of lignosulfonate concentration in water (no added salt) as measured by pendant drop tensiometry.

comparison, which led to the testing of NaCl, $CaCl_2$ and $AlCl_3$. The dependence of interfacial storage and loss modulus on concentration of these added electrolytes is also plotted in Fig. 6. The curves are qualitatively similar, each showing an almost parallel progression of storage and loss modulus with a local maximum. With increasing charge number of the cation, this maximum is moved towards lower salt concentrations. In addition, the storage modulus increases in value. Compared to no added salt, $AlCl_3$ increased the maximum storage modulus by almost one magnitude. This is evidence for a strong effect of multivalent cations on the viscoelastic properties of interfacial lignosulfonate films. These findings are in agreement with previous studies [14,27], which stated increased rigidity for lignosulfonate films formed in presence of multivalent cations.

Exemplary results obtained from the strain sweeps are plotted in Fig. 7. As can be seen, the interfacial layer is broken up at a strain of approximately 1 %. This process is marked by a decrease of interfacial modulus, which is in some cases preceded by a temporary increase. Both interfacial storage and loss modulus remained constant below a strain of approximately 0.5 %, which represents the linear viscoelastic range. The chosen strain of 0.2 % was within this range for all experiments. Equilibration period and frequency sweep were therefore conducted without irreversibly deforming the interfacial film. Data points were omitted, which were below the minimum torque required for the shear rheometer. Because of this, some of the curves in Fig. 7 start at a higher strain, even though all samples were tested according to the same protocol.

The strain sweep in Fig. 7 also shows an increase of interfacial storage modulus with increasing cation charge number, which is in coherence with both Figs. 6 and 8. In addition, Fig. 8 shows that the qualitative progression of storage and loss modulus relative to each other could be different. In case of no added salt, the data points of storage and loss modulus were approaching each other with increasing

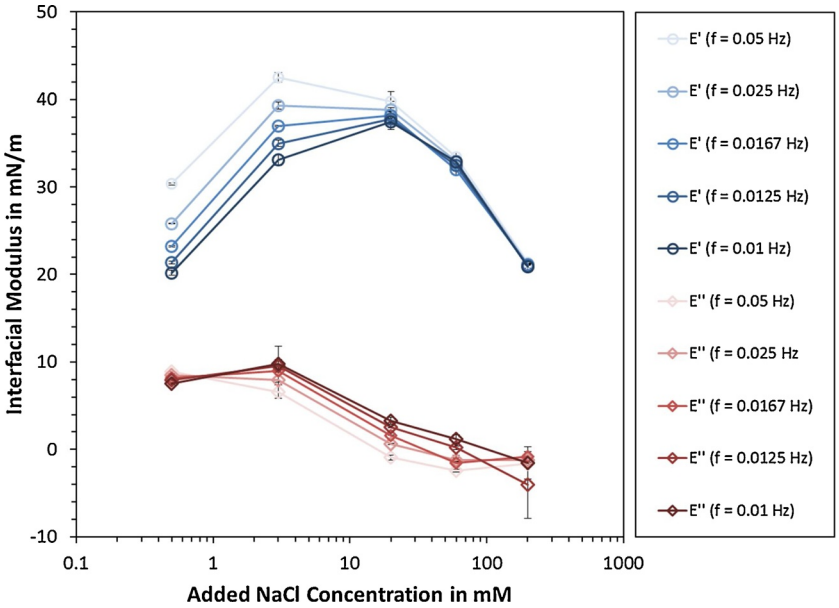

Fig. 5. Interfacial moduli of 1.8 g/l lignosulfonate in water in dependence of added NaCl concentration as measured by pendant drop tensiometry.

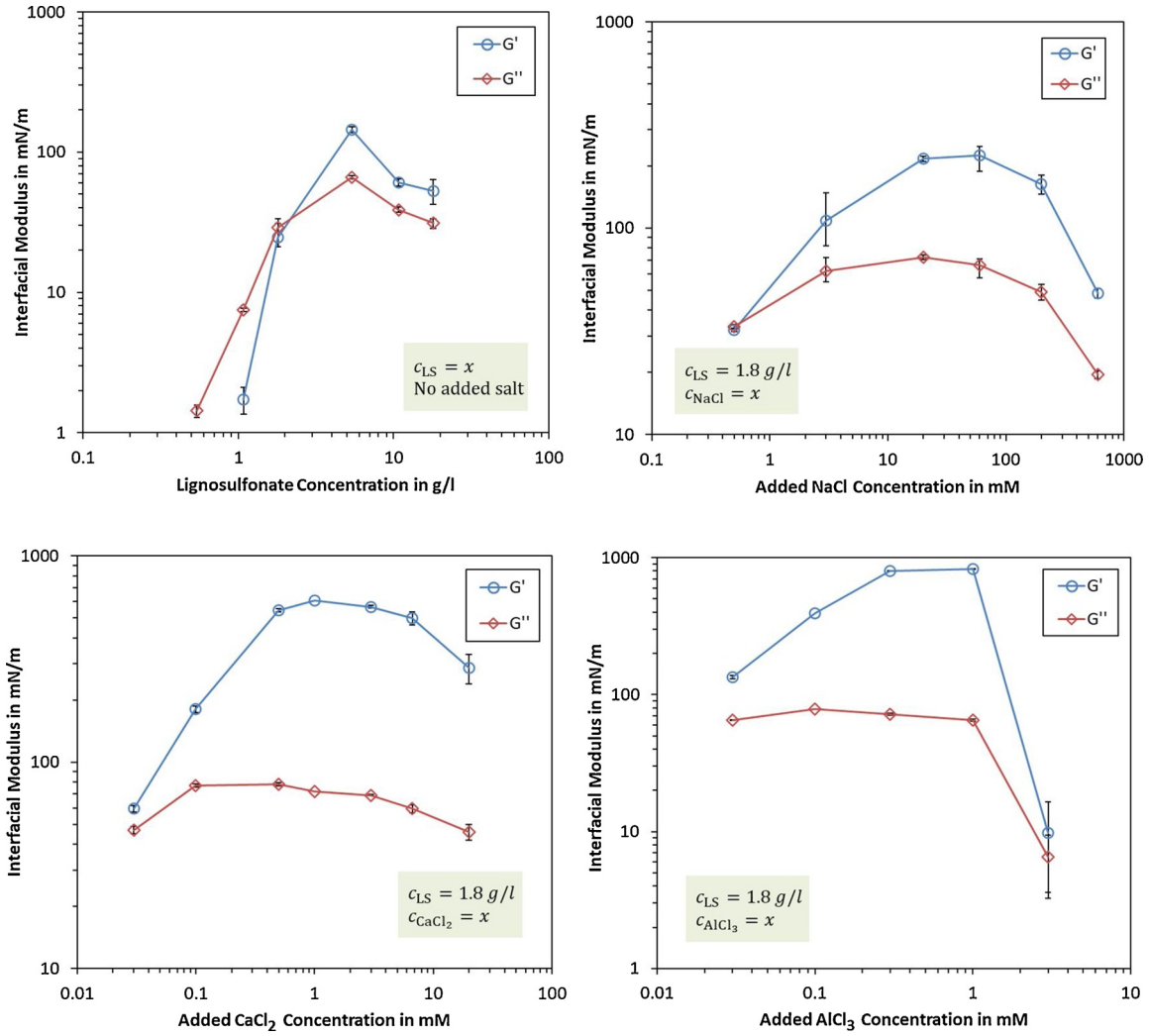

Fig. 6. Interfacial moduli in dependence of lignosulfonate or added salt concentration as measured by interfacial shear rheology.

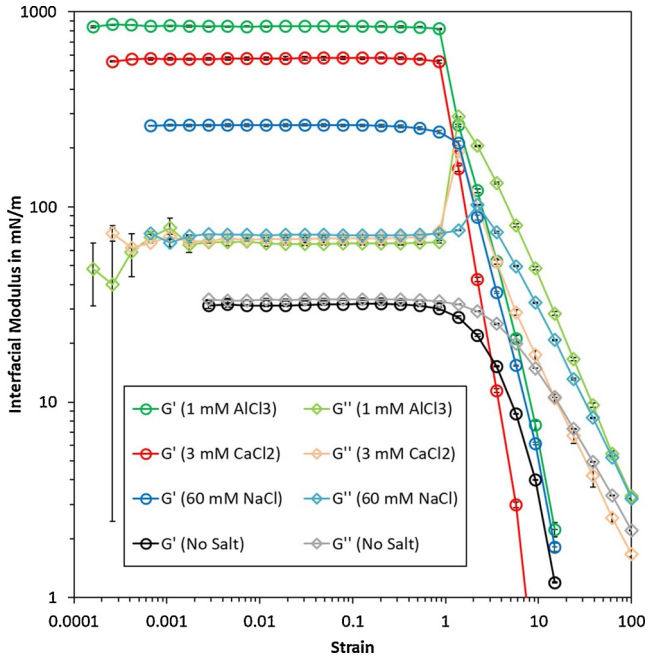

Fig. 7. Strain sweep of 1.8 g/l lignosulfonate with different salts in water and xylene at the water-oil interface at 1 Hz.

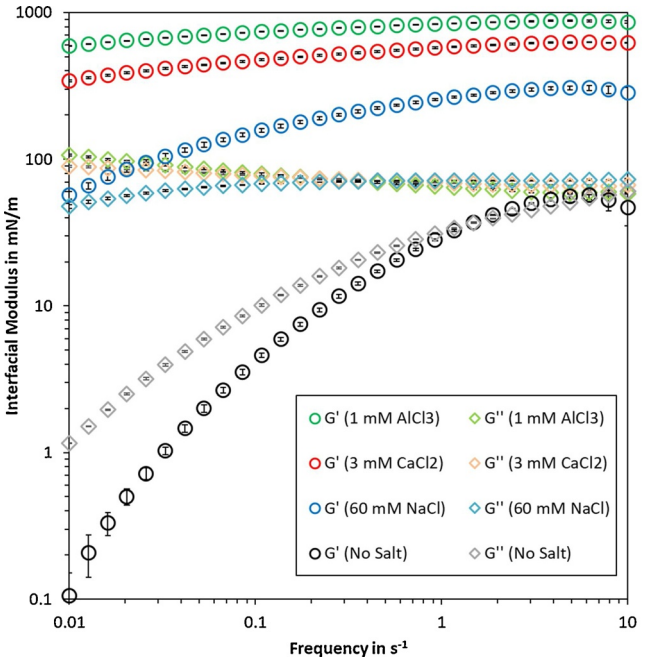

Fig. 8. Frequency sweep of 1.8 g/l lignosulfonate and different added salts at 0.2 % strain.

frequency and intersected at 1.5 Hz. This behavior is characteristic for viscoelastic interface films. After addition of NaCl, the two curves are no longer intersecting within the tested range of 0.01–10 Hz. Still, the curves would intersect if extrapolated below 0.01 Hz. In contrast to that, the samples with added $CaCl_2$ or $AlCl_3$ exhibit moduli that are further far apart with no tendency to intersect. These storage and loss moduli are in an almost parallel arrangement, which is characteristic for that of gelled interfaces. Evidence is therefore given that di and trivalent metal ions can induce interfacial gelling of lignosulfonate. Such behavior could be explained by metal ion-lignosulfonate complexation, in which the anionic functional groups between lignosulfonate molecules are bridged by the multivalent metal ions. Similar mechanisms were described e.g. for interactions between calcium and polyacrylate or polyelectrolyte induced flocculation of colloidal dispersions [52–54].

3.3. Lignosulfonate salting out and comparison with interfacial shear rheology

Salting out experiments were conducted to link the interfacial properties and the dispersion state. The salt concentrations were adjusted to match the data of interfacial shear rheology. The measured data was further converted to the percentage of lignosulfonate removed after centrifugation LS_c and after filtration LS_f, as given by Eqs. (8) and (9), respectively. Here, c_0 refers to the initial lignosulfonate concentration, $c_{aq,c}$ to the concentration after centrifugation and $c_{aq,f}$ to the concentration after filtration.

$$LS_c = 1 - \frac{c_{aq,c}}{c_0} \tag{8}$$

$$LS_f = \frac{c_{aq,c} - c_{aq,f}}{c_0} \tag{9}$$

The results are listed in Table 1. As can be seen, centrifugation would only decrease the lignosulfonate bulk concentration at the highest and second highest concentration of $CaCl_2$ or $AlCl_3$. The concentration was consistently lower after filtration than after centrifugation, which shows that part of the lignosulfonate was always retained by the filter. In case of $CaCl_2$ and $AlCl_3$ addition, the percentage retained by filtration showed a maximum, which preceded the increase in lignosulfonate removed by centrifugation. It therefore appears that lignosulfonate agglomerate growth preceded the precipitation onset. Before precipitation onset, the concentration after centrifugation was within 1.80 ± 0.01 g/l. Percentages removed or retained were hence only calculated if surpassing the experimental error of 0.01 g/l.

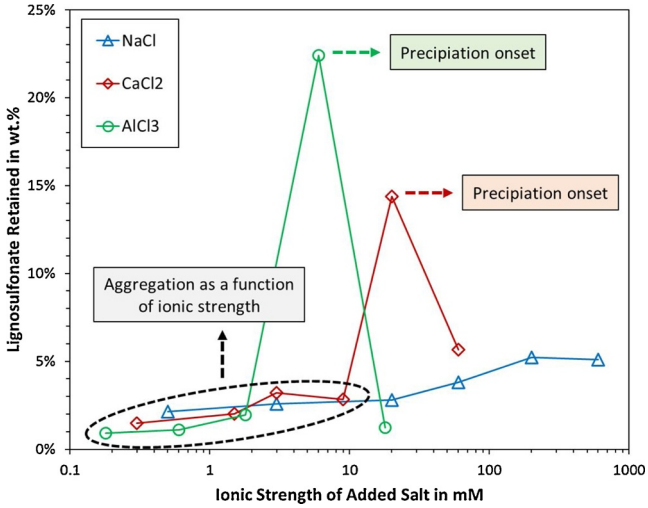

Fig. 9. Lignosulfonate retained by filtration in dependence of ionic strength of added salts. Three different salts were tested at 1.8 g/l lignosulfonate in aqueous solution.

When plotting lignosulfonate retained by filtration versus ionic strength as in Fig. 9, the graphs appear to align below precipitation onset. Filtration is a rather crude way of quantifying lignosulfonate agglomeration and this plot neglects, for example, the contribution of the lignosulfonate to the ionic strength. However, the ion contribution of the lignosulfonate would be constant for all three cases, yielding the same alignment of the graphs with respect to each other. At the bottom line, it appears that lignosulfonate agglomeration is driven by ionic strength, but more data would be needed to confirm this.

The measured concentrations were plotted in Fig. 10 together with the storage modulus obtained by interfacial shear rheology. All three salts exhibit the same trend, in which a decrease in interfacial storage modulus is coinciding with salting out or preceded by it. Destabilization of the lignosulfonate from solution, i.e. by precipitation or agglomerate growth, therefore aligned with destabilization of the interfacial film. One of the reasons for this behavior could be that precipitation reduced the bulk concentration, which further diminished the driving force behind lignosulfonate adsorption at the interface. In case of NaCl, a decreasing interfacial modulus is coinciding with 5 wt.% or more of lignosulfonate retained by filtration. Enhanced lignosulfonate aggregation could therefore disturb the arrangement of adsorbed

Table 1
Salting out of 1.8 g/l lignosulfonate from aqueous solution.

		After centrifugation		After filtration	
Salt Type	Salt concentration	Lignosulfonate concentration	Lignosulfonate removed	Lignosulfonate concentration	Lignosulfonate retained
	mM	*g/l*	*wt.%*	*g/l*	*wt.%*
NaCl	0.5	1.80	–	1.76	2.1
	3	1.80	–	1.75	2.6
	20	1.80	–	1.75	2.8
	60	1.80	–	1.73	3.8
	200	1.81	–	1.71	5.2
	600	1.80	–	1.71	5.1
$CaCl_2$	0.1	1.81	–	1.79	1.5
	0.5	1.81	–	1.78	2.0
	1	1.80	–	1.74	3.2
	3	1.79	–	1.74	2.8
	6.67	1.78	1.4	1.52	14.4
	20	0.83	54.0	0.73	5.7
$AlCl_3$	0.03	1.80	–	1.78	0.9
	0.1	1.80	–	1.78	1.1
	0.3	1.80	–	1.77	2.0
	1	1.46	19.0	1.05	22.4
	3	0.20	88.7	0.18	1.2

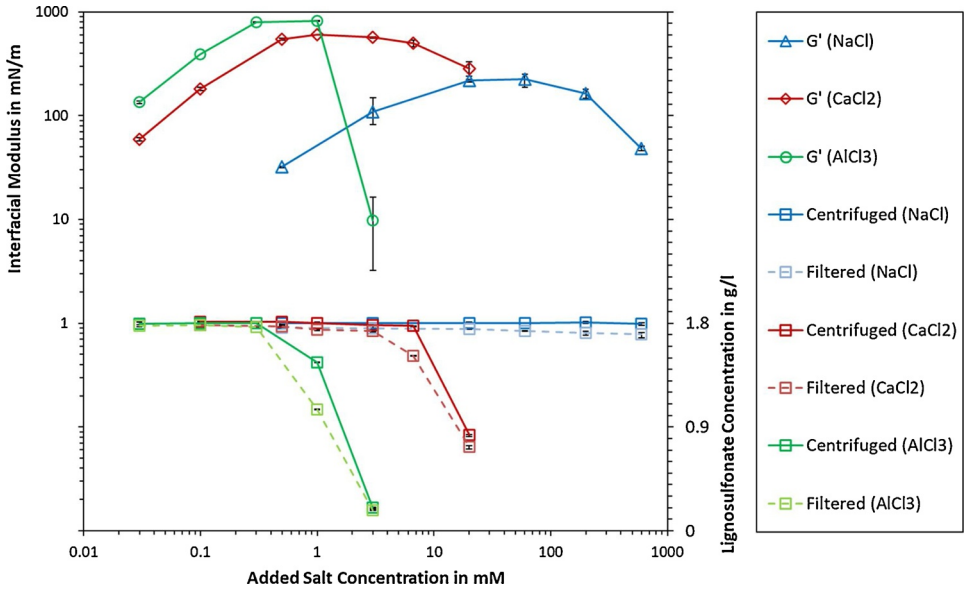

Fig. 10. Comparison of interfacial shear rheology and salting out experiments of 1.8 g/l lignosulfonate at various salt concentrations.

lignosulfonate at the interface. An additional explanation would be that electrolyte contraction at high ionic strength could reduce the attractive forces between lignosulfonate molecules and aggregates. A detailed discussion is given in Section 3.6. The developed separation procedure was also limited, because the filter had a finite pore size (0.2 μm), which would allow smaller aggregates to pass. Still, the NaCl experiments agree with the trend observed for $CaCl_2$ and $AlCl_3$, where the maximum of interfacial modulus is coinciding with the onset of lignosulfonate destabilization from solution.

3.4. Effect of salt addition on lignosulfonate emulsion stabilization

Emulsion stability was studied for varying $CaCl_2$ and $AlCl_3$ concentration, since no lignosulfonate precipitation was observed within the tested NaCl concentration. Four different cases were identified with respect to interface properties and lignosulfonate dispersion state:

(a) No added salt, yielding low interfacial modulus and no interfacial gelling.
(b) Low amount of added salt, which increased the interfacial modulus without inducing interfacial gelling.
(c) Intermediate amount of added salt, inducing interfacial gelling and a storage modulus close to the maximum.
(d) High amount of added salt, which induced lignosulfonate precipitation and reduced the interfacial modulus.

These cases were tested for xylene in water emulsions at two oil/water ratios. The results are plotted in Fig. 11, where less oil recovered accounted for better emulsion stability. As expected, emulsion stability increased when going from no added salt (a) to low amount (b) and further to intermediate amount of added salt (c). The dispersion state of lignosulfonate was most significantly changed for case (d). Here, the lignosulfonate is mostly found as dispersed particles. The dominant stabilization mechanism is hence changed from adsorption to the formation of a Pickering-emulsion. As a result, emulsion stability in case (d) tended to be lower than in case (c), especially at the higher oil/water ratio of 60/40, where full coverage of emulsified droplets with the particles is more difficult.

The trends observed from emulsion destabilization were not unexpected. Two principles have long been established, which state that droplet coalescence can be prevented by viscoelastic interface films and that stability is usually beset when the stabilizing agents are on the

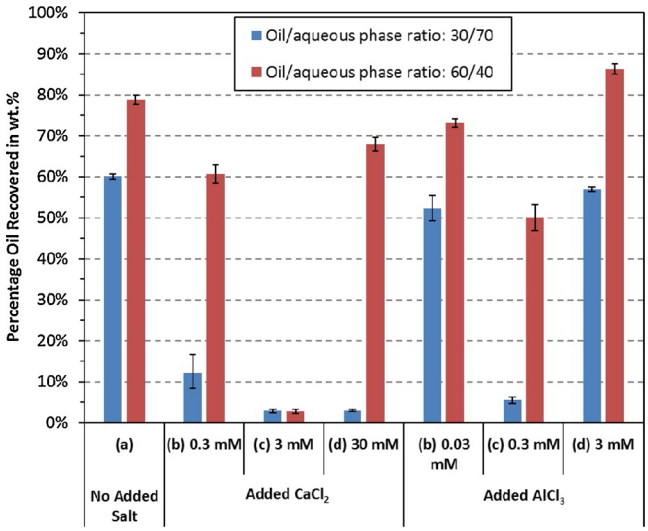

Fig. 11. Emulsion stability for different volumetric ratios of xylene emulsified in water with 1.8 g/l lignosulfonate and added salt at different concentrations.

verge of precipitation [35,55]. Fig. 11 is therefore coherent with the data from interfacial rheology. In a more general context, this also highlights the implication that should be drawn for technical applications: Lignosulfonates are best utilized in high salinity environments, where lignosulfonate precipitation imminent but not apparent.

3.5. Modelling considerations

3.5.1. Surface excess

The results from pendant drop tensiometry were used to calculate several physical properties. Firstly, the surface excess was determined via the dependence of equilibrium interfacial tension on lignosulfonate concentration, as plotted in Fig. 3. It is widely established that this linearlogarithmic region can be fitted using Gibbs adsorption isotherm [56]. As shown in Eq. (10), the surface excess Γ_m is a function of the change in interfacial tension γ over the change in logarithmic lignosulfonate concentration c_{LS}. The gas constant R, the temperature T, and the constant n are further involved in this calculation.

Table 2
Surface excess, area per molecule, and equilibration constant as determined by pendant drop tensiometry.

Parameter	Unit	Values				
Constant n	–	1	2	4	8	16
Surface excess Γ_m	$^{mol}/_{m^2}$	1.23×10^{-6}	6.14×10^{-7}	3.07×10^{-7}	1.53×10^{-7}	7.67×10^{-8}
	$^{mg}/_{m^2}$	2.21	1.11	0.55	0.28	0.14
Area per molecule A_m	Å	135	270	541	1082	2164

$$\Gamma_m = -\frac{1}{nRT}\left(\frac{\partial\gamma}{\partial \ln c_{LS}}\right) \tag{10}$$

It holds that $n = 1$ for nonionic surfactants or ionic surfactants in presence of excess electrolyte. Assuming electrical neutrality at the interface, one can further assume $n = 2$ for 1:1 ionic surfactants [57]. In case of polyelectrolytes, however, the value for n is less trivial. Effective charge numbers between 2–22 have been reported for lignosulfonates [12,58]. The molecular weight of the lignosulfonate used in this study was comparably low, which makes charges numbers between 2–8 most realistic. The surface excess was calculated for values of $n = 1...16$ and the results are listed in Table 2. In addition, the area per molecule A_m was computed using the Avogadro's constant N_{av} as in Eq. (11). All calculations used the lignosulfonate's number average molecular weight of $M_n = 1800\frac{g}{mol}$.

$$A_m = \frac{1}{\Gamma_m N_{av}} \tag{11}$$

In a previous publication, we determined the surface excess for this lignosulfonate sample to be $\Gamma_m = 7.50 \times 10^{-7}\frac{mol}{m^2} \approx 1.35\frac{mg}{m^2}$ [45]. The previous experiments were conducted at high salinity (0.6 M NaCl), which simplified the calculations since $n = 1$ due to excess electrolyte. Comparing our previous results with Table 2, it is obvious that $n = 2$ provides values closet to the previously measurement. Using such a convention, the surface excess in this publication ($1.11\frac{mg}{m^2}$) would be slightly lower than the previously reported value ($1.35\frac{mg}{m^2}$) at high salinity. This would be expected, as high salinity yields a compression of the electrostatic repulsion layer, which would facilitate the adsorption of a larger amount of lignosulfonate at the interface. Subsequent calculations were therefore conducted using $n = 2$, as this convention was deemed the most realistic case.

Previous reports have stated that lignosulfonate adsorption follows the Langmuir isotherm [18–20]. The surface excess Γ can thus be described via Eq. (12), that is, as a function of the lignosulfonate concentration c_{LS}, the Langmuir equilibration constant K, and the maximum adsorbed surfactant concentration Γ_∞. In this case, Γ_∞ is equal to Γ_m.

$$\Gamma = \frac{\Gamma_\infty K c_{LS}}{1 + K c_{LS}} \tag{12}$$

Langmuir type adsorption further implies the applicability of the Szyszkowski Eq. (13). Here, the surface pressure Π is computed as difference of interfacial tension γ at specific lignosulfonate concentration and the interfacial tension γ_0 of the pure solvents, which was determined as $\gamma_0 = 35.3\frac{mN}{m}$ from blank experiments. The Szyszkowski equation was further rearranged to compute the Langmuir equilibration constant K.

$$\Pi = \gamma_0 - \gamma(c_{LS}) = nRT\Gamma_m \ln(1 + K c_{LS}) \tag{13}$$

Combining the data of Fig. 3 and Table 2 yielded an average equilibration constant of $K = 459\frac{m^3}{mol}$. This value should be interpreted with care, however, as the curvature of the graph is poorly described by the experimental data. It must be noted that the equilibrium constant K is independent of different values for n due to the product term $n \times \Gamma_m$ in the Szyszkowski equation. The experimental data and model fits were plotted in Fig. 12.

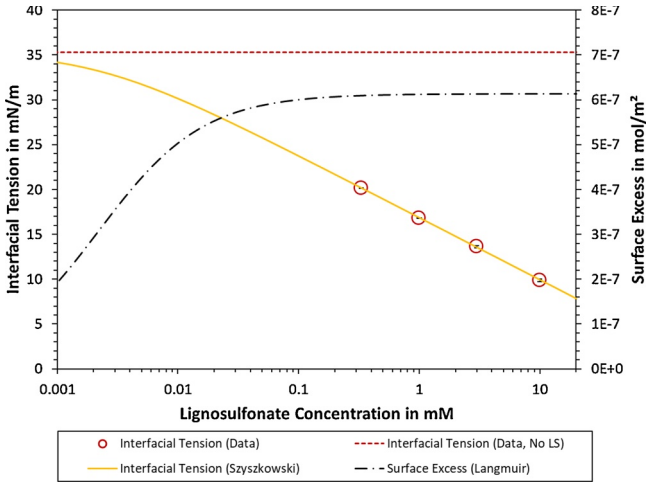

Fig. 12. Interfacial tension data of lignosulfonate in water (no added salt), surface excess, and model fits according to Langmuir and Szyszkowski equation.

3.5.2. Diffusion coefficient

The previous sub-section (3.5.1) was concerned with equilibrated data of interfacial tension to calculate the surface excess. In this chapter, the dynamics of interfacial adsorptions are considered to estimate the diffusion coefficient.

In a simplified model view, the interface has no adsorbed material at its creation ($t = 0$). Following the creation of the new interface, the surfactant is diffusing from the bulk solution towards the interface to adsorb. Two mechanisms have been proposed to describe this adsorption [57]: (1) a diffusion-controlled model and (2) mixed kineticdiffusion. Model (2) assumes that the rate controlling step is at the interface, i.e. an energy barrier must be overcome for molecules to adsorb. Model (1) on the other hand assumes that only mass transport is rate limiting. Ward and Todai proposed a model to describe the surface excess for such diffusioncontrolled processes [59]. This model included two asymptotic cases, which are a short-time ($t \to 0$) and a long-time ($t \to \infty$) approximation. The short-time approximation requires the interfacial tension to be close to the pure component interfacial tension ($\gamma_{dyn} \to \gamma_0$). This prerequisite was not met by the data in this article, as the initial adsorption proceeded too rapid to be measured by the pendant drop technique at the tested concentrations. The short-time approximation could consequently not be used. The long-time approximation assumes that enough time has passed for the subsurface concentration to be equal to the bulk concentration. This condition was fulfilled, as the presented data was sufficiently equilibrated. The dynamic interfacial tension γ_{dyn} is given in Eq. (14) according to the long-time approximation, which is a function of the diffusion coefficient D, time t, and the equilibrated interfacial tension γ.

$$\gamma_{dyn} = \gamma + \frac{nRT\Gamma_m}{c_{LS}}\sqrt{\frac{\pi}{4Dt}} \tag{14}$$

Linear regression was performed on the data of the interfacial tension γ_{dyn} in dependence of $\frac{1}{\sqrt{t}}$ at $t \to 5h$. The intervals for regression were manually set to only comprise data that progressed linearly. As can be seen in Fig. 13, the regression line is a close fit to the data at the asymptotic condition (left-hand-side plot). As a result, the model fit was equivalently good for unmodified data close to the equilibrium (right-hand-side plot).

The regression lines from Fig. 13 were used to compute the apparent diffusion coefficient. This was done by equating the slope of the regression line with $\frac{nRT\Gamma_m}{c_{LS}}\sqrt{\frac{\pi}{4D}}$, as is given in Eq. (14), and further solving

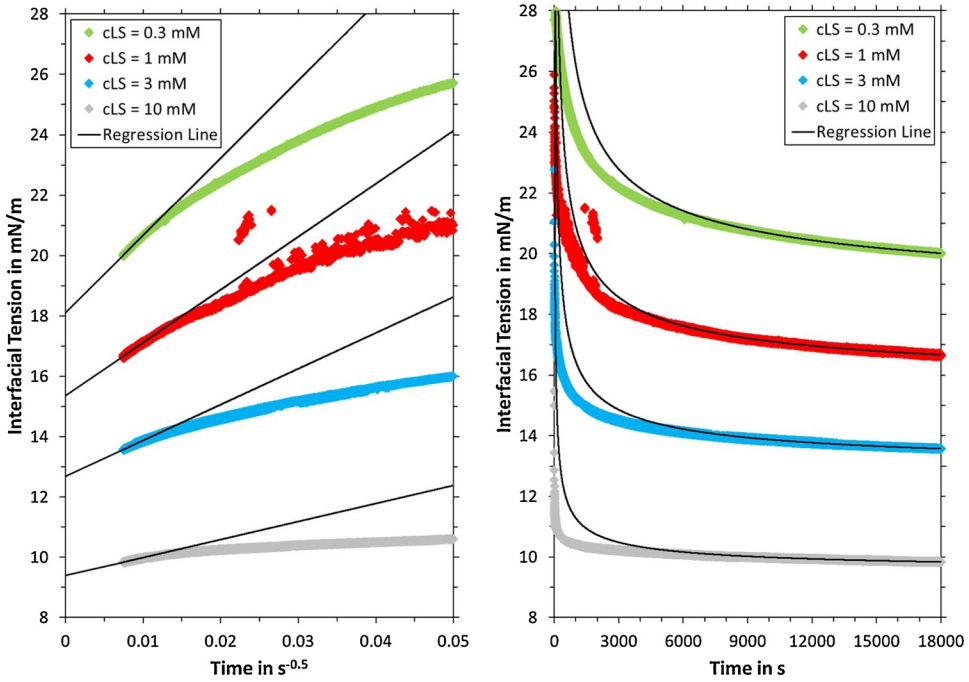

Fig. 13. Interfacial tension and regression lines of Ward and Todai long-time approximation of aqueous solutions of lignosulfonate (no added salt). The graphs were plotted as a function of one over square root of time (left-hand-side) or without modification (right-hand-side).

for D.

The apparent diffusion coefficient D was plotted as a function of lignosulfonate concentration in Fig. 14. As can be seen, the diffusion coefficient is decreasing with increasing lignosulfonate concentration. Such behavior is typical for colloidal dispersions, in which the surfactant undergoes selfassociation. Sztukowski and Yarranton observed similar behavior of petroleum asphaltenes when studying interfacial dynamics [50]. Based on their work, the authors proposed Eq. (15) to describe the apparent diffusion coefficient D as a function of asphaltene concentration c_2. The terms a and b are fitting constants.

$$D = ac_2^b \tag{15}$$

Eq. (15) was found applicable for our data in Fig. 14. Using $c_2 = c_{LS}$, the best model fit was obtained for a and b being equal to 8.26×10^{-17} and -1.07, respectively.

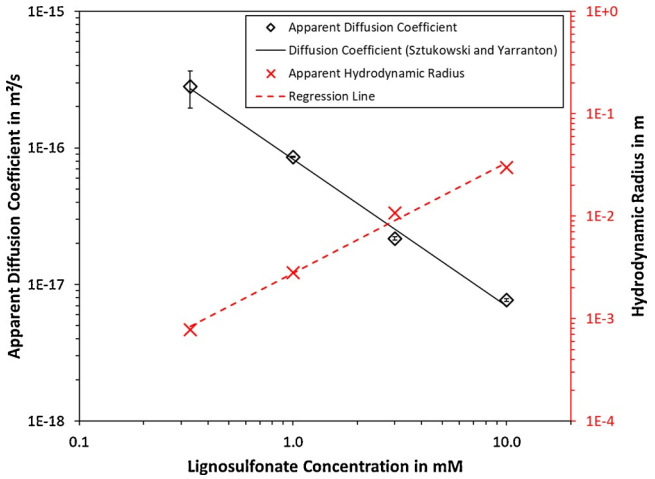

Fig. 14. Diffusion coefficient determined by long-time approximation (Warde and Todai) fitted with the regression model proposed by Sztukowski and Yarranton. The hydrodynamic radius was plotted in addition, as obtained from the diffusion coefficient by Einstein-Stokes equation. Error bars mark the min/max values of the measured data.

In addition, the diffusion coefficient allows the computation of the hydrodynamic radius R_H via the Einstein-Stokes relation [60], as shown in Eq. (16). Additional terms involved are the Boltzmann constant k_B and the viscosity η.

$$R_H = \frac{k_B T}{6\pi\eta D} \tag{16}$$

Calculating the apparent hydrodynamic radius revealed that the data in Fig. 14 must be interpreted with care. The values suggest particles within the range of several millimeters and larger. Such particles were indeed not observed. The solutions with only lignosulfonate exhibited no signs of precipitation, in contrast to e.g. solutions containing lignosulfonate and high concentrations of multivalent cations. The diffusion coefficient of lignosulfonates was determined experimentally by Kontturi [58], who measured values between 0.84 to $1.58 \times 10^{-10}\frac{m^2}{s}$ at 20 °C. The apparent diffusion coefficients in Fig. 14 are therefore likely an underestimate, which would further exaggerate the values for the hydrodynamic radius. The assumption of a diffusion-controlled mechanism is hence insufficient. We will further compare with results of other authors, who modelled the behavior of petroleum asphaltenes. Pradilla et al. applied the model by Ward and Todai to solutions of asphaltene ($M_w \approx 750\frac{g}{mol}$) or Brij 93 ($M_w \approx 357\frac{g}{mol}$), yielding short-time diffusion coefficients as low as $2.15 \times 10^{-18}\frac{m^2}{s}$ (asphaltenes) and long-time diffusion coefficients as low as $2.35 \times 10^{-15}\frac{m^2}{s}$ (Brisj 93) [61]. Nenningsland et al. fitted the Lucassen and van den Tempel (LvdT) model with interfacial rheology data from asphaltene solutions, for which the best fit was obtained at diffusion coefficients in the range of 10^{-13} to $10^{-17}\frac{m^2}{s}$ [62]. The results in Fig. 14 are therefore coherent with the work of other authors, who applied models with similar assumptions.

Based on the results in this section, it is concluded that lignosulfonate adsorption at the water-oil interface is not diffusion-controlled at the considered time scale. We propose that a mixed-kinetic diffusion model could provide more realistic modelling results, for example by including a potential energy barrier for adsorption. In addition, phenomena such as competitive adsorption and conformation

changes of lignosulfonate molecules at the interface could be accounted for. The findings do, however, not rule out applicability of a diffusion-controlled mechanism on the short time scale. Furthermore, it was found that lignosulfonate aggregation can affect interfacial adsorption, as the diffusion coefficient was dependent on lignosulfonate concentration.

3.5.3. Interfacial Modulus

As introduced in Eq. (3), the complex interfacial modulus E^* is the sum of the contributions from the elastic modulus E' and the viscous modulus E''. The LvdT model was developed to describe these moduli for dilatational interfacial rheology conducted at low frequency, that is, below 0.1 Hz [63]. In addition, the assumptions of reversible and diffusion-limited adsorption are made by this model. The LvdT model proposes that E' and E'' are calculated from the instantaneous elasticity E_0 and the dimensionless parameter Ω, as shown in Eq.s (17) and (18).

$$E'(\omega) = E_0 \frac{1+\Omega}{1 + 2\,\Omega + 2\Omega^2} \tag{17}$$

$$E''(\omega) = E_0 \frac{\Omega}{1 + 2\,\Omega + 2\Omega^2} \tag{18}$$

The instantaneous elasticity E_0 is defined as in Eq. (19).

$$E_0 = \frac{d\gamma}{d\Gamma}\Gamma \tag{19}$$

The term Ω is a function the diffusion coefficient D and the change in concentration by surface excess, as in Eq. (20). Furthermore, the pulsation ω is a function of the oscillation period τ (Eq. (21)).

$$\Omega = \frac{dc_{LS}}{d\Gamma}\sqrt{\frac{D}{2\omega}} \tag{20}$$

$$\omega = \frac{2\pi}{\tau} \tag{21}$$

To compute the terms $\frac{d\gamma}{d\Gamma}$ and $\frac{dc_{LS}}{d\Gamma}$, the Langmuir equation and the Szyszkowski equation are assumed. Linking the surface excess Γ with the interfacial tension γ or the bulk concentration c_{LS} leads to the derivation of Eqs. (22) and (23) [51].

$$E_0 = nRT\Gamma_m K c_{LS} \tag{22}$$

$$\Omega = -\frac{1}{K}\left(\frac{1}{\Gamma-\Gamma_m} - \frac{\Gamma}{(\Gamma-\Gamma_m)^2}\right)\sqrt{\frac{D}{2\omega}} \tag{23}$$

The LvdT model was solved using the parameters determined in subsections 3.5.1 and 3.5.2, however, the model did not match the experimental data sufficiently. To obtain a better fit, an iterative approach was chosen. Using $n = 2$ and $\Gamma_m = 6.14 \times 10^{-7}\frac{mol}{m^2}$, the parameters K and D were determined by minimizing the sum of errors squared, as in Eq. (24).

$$\sum_i^n (E'_{model,i}(K, D) - E'_{data,i})^2 + \sum_i^n (E''_{model,i}(K, D) - E''_{data,i})^2 \equiv \min \tag{24}$$

The best model fit is plotted in Fig. 15. As can be seen, the elastic modulus E' of the model qualitatively matches the experimental data. The LvdT model could therefore be used to explain the observed trends. That is, increasing the lignosulfonate concentration would initially increase the elastic modulus due to rising surface coverage. At high lignosulfonate concentration, the mass transport would be enhanced due to higher availability of lignosulfonate molecules, which would further reduce the elastic modulus, as for example empty sites are filled more quickly during interface expansion. The LvdT model also provides an explanation for the dependency of elastic modulus on oscillation period or frequency. At longer periods, the molecules would be given more time to diffuse from and to the interface, which would reduce the observed elastic modulus.

The model fit of the viscous modulus E'' was not matching, both qualitatively and quantitatively, which suggests that there are shortcomings in modelling the interfacial behavior of lignosulfonates via LvdT. As concluded in sub-section 3.5.2, the assumption of a diffusion-controlled mechanism was most likely insufficient. This was further supported by non-matching Langmuir equilibration constants. From LvdT it was determined that $K = 9.127\frac{m^3}{mol}$, which was 50times lower than the value obtained by fitting the Szyszkowski equation in subsection 3.5.1. The apparent diffusion coefficient D, on the other hand, was determined as $1.4 \times 10^{-17}\frac{m^2}{s}$, which is within the estimations from the Ward and Todai model. This supports the results from subsection 3.5.2 and the conclusion that lignosulfonates are undergoing interfacial adsorption in an aggregated state.

3.6. Discussion and generalized view

The detailed characterization of interfacial lignosulfonate films and bulk behavior, as given in this article, was further used to explain the results by a generalized model view.

3.6.1. Ionic strength

As shown in Section 3.1, increasing lignosulfonate or NaCl concentration yielded a logarithmic decrease of (equilibrated) interfacial tension. Naturally, a higher bulk concentration will yield lower interfacial tension, as bulk excess of surfactant would shift the equilibrium thermodynamics towards more adsorption. NaCl addition showed the same relationship, which suggests that increasing salinity is a key driving factor of interfacial adsorption. It has been shown that counterion condensation is facilitated by increasing lignosulfonate concentration [12]. Reducing the electrostatic repulsion layer around lignosulfonate molecules would indeed yield a closer packing of molecules at the interface. In addition, Fig. 9 showed an almost linear correlation of ionic strength with the amount of lignosulfonate retained by filtration. It is therefore clear that lignosulfonate interactions with hydrophobic materials are promoted by increasing ionic strength. This would include both the interactions with interfaces as well as lignosulfonate self-assembly.

We furthermore propose that, on a molecular basis, lignosulfonate is affected in the same manner by increasing lignosulfonate concentration as it is by increasing the NaCl concentration. This assumption is fundamental to explaining the measured interfacial moduli. Increasing the sodium lignosulfonate or NaCl concentration had the same effect on the interfacial modulus in Sections 3.1 and 3.2. Lignosulfonate aggregation was only measured for increasing NaCl concentration, but other reports revealed that aggregation can also occur as a result of increasing lignosulfonate concentrations, for example as evidenced by surface tension measurements [22,23]. One could therefore assume that lignosulfonate aggregation at high lignosulfonate concentration is occurring in a similar manner as NaCl induced aggregation. Apart from that, the polyelectrolyte expansion of lignosulfonates at low concentration is a function of ionic strength, which is independent of the type of added electrolyte [64].

3.6.2. Monovalent cations

Figs. 4 and 5 showed a maximum of interfacial modulus at intermediate lignosulfonate or NaCl concentration. The modulus decreased at higher concentration. One explanation for such behavior was given in Section 3.5.3. Following the LvdT model, the mass transport at high surfactant concentrations is as fast as that the viscoelastic response of the interface is reduced. For example, empty sites at the interface arising during expansion are filled faster, which would reduce the delay of changing interfacial tension and hence the elastic modulus. However, it was concluded that interfacial behavior of lignosulfonates is not diffusion controlled, so this explanation has only limited validity. In addition, diffusional mass transfer cannot explain the interfacial moduli in Fig. 6, as the surface area of the interface did not change during

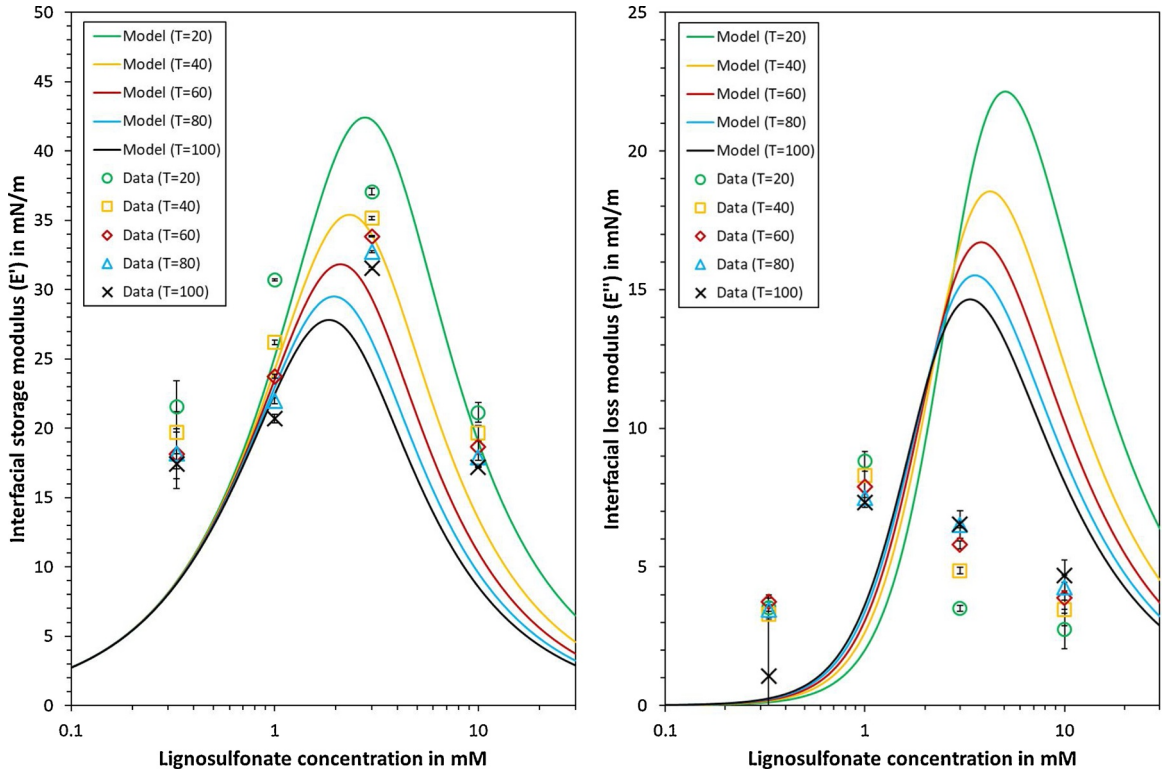

Fig. 15. LvdT model fit obtained after least squares regression of the interfacial moduli in dependence of lignosulfonate concentration (no added salt). The fitting parameters were determined as $K = 9.127\frac{m^3}{mol}$ and $D = 1.4 \times 10^{-17}\frac{m^2}{s}$ using $n = 2$ and $\Gamma_m = 6.14 \times 10^{-7}\frac{mol}{m^2}$.

interfacial shear rheology. Here, an increase in concentration should in theory yield an increasing or constant interfacial modulus, as the surface coverage does not change during the measurement.

As shown in Fig. 10, the interfacial modulus started decreasing at salt concentrations that invoked lignosulfonate precipitation or enhanced aggregation. The interfacial behavior of lignosulfonates therefore appeared to be linked to the aggregation state. One could argue that the decrease in elastic modulus is linked to the increasing spatial dimensions of the aggregates, which could, for example, disturb an orderly arrangement of molecules at the interface. However, we disagree with this explanation, because it would entail an increase in viscous modulus, which was not observed.

Based on the decrease in elastic modulus, a loss in intermolecular or interaggregate cohesion at high ionic strength is evident. The attractive forces between lignosulfonates molecules or aggregates include effects such as hydrogen bonding and π-interactions [11,65]. The repulsive forces are dominated by electrostatic repulsion of the anionic groups. These coulomb forces also account for polyelectrolyte expansion of individual lignosulfonate molecules [64,66]. As ionic strength increases, charge screening results in reduced spatial dimensions of the lignosulfonate molecules and aggregates. In addition, ionized groups in the center of lignosulfonate aggregates can attain charge neutrality faster at high salinity [67], which would yield a further collapse of the aggregate. We propose that this collapse or compaction inhibits attractive interactions. As the dimensions of lignosulfonate aggregates are reduced, a concentration of hydrophilic functional groups would occur on the aggregate surface. This would sterically shield the more hydrophobic groups, such as aromatic ring structures, which are responsible for attractive π-interactions. A loss of cohesion of the interfacial film would ultimately be the result, as the sites for intermolecular or interaggregate attraction are diminished. A schematic of the proposed mechanism is shown in Fig. 16.

Compaction of lignosulfonate aggregates can conveniently explain the observed decrease of interfacial modulus, while still accounting for decreasing interfacial tension at increasing lignosulfonate or salt concentration. This interpretation is in agreement with the results of Vainio et al., who showed that strong interparticle association was encompassed by only a slight decrease of surface charge [12]. It could also explain the increase in distance between lignosulfonate aggregates at 0.2 M NaCl, as compared to a saltfree solution [11].

3.6.3. Di- and trivalent cations

Intermolecular bridging of multivalent cations is an additional effect that changes the interfacial characteristics of lignosulfonates. As evidenced by Fig. 8, the presence of calcium or aluminum ions could induce interfacial gelling. It is therefore no surprise that the maximum interfacial storage modulus was 4.2 (calcium) and 5.7 (aluminum) times larger, as compared to no added salt in Fig. 6. However, the decrease of interfacial modulus occurred at lower ionic strength for calcium and aluminum than for sodium. We therefore propose that polyelectrolyte compaction, as discussed in sub-section 3.6.2, is not the main cause for the trend in elastic modulus. Instead, precipitation reduces the effective bulk concentration. At lower concentration, less lignosulfonate is adsorbed at the interface reducing surface coverage and ultimately the interfacial modulus.

4. Summary and conclusion

In this article, the viscoelastic properties of interfacial lignosulfonate films were studied with respect to lignosulfonate concentration and salinity. Both dilatational interfacial rheology and interfacial shear rheology were adapted for this purpose. In addition, lignosulfonate salting out and effect of salinity on emulsion stability were investigated.

Our results show, for the first time, conclusive proof of interfacial gelling of lignosulfonates in presence of di- and trivalent cations. As interfacial shear rheology revealed, the presence of calcium or aluminum ions also yielded higher interfacial storage modulus, as

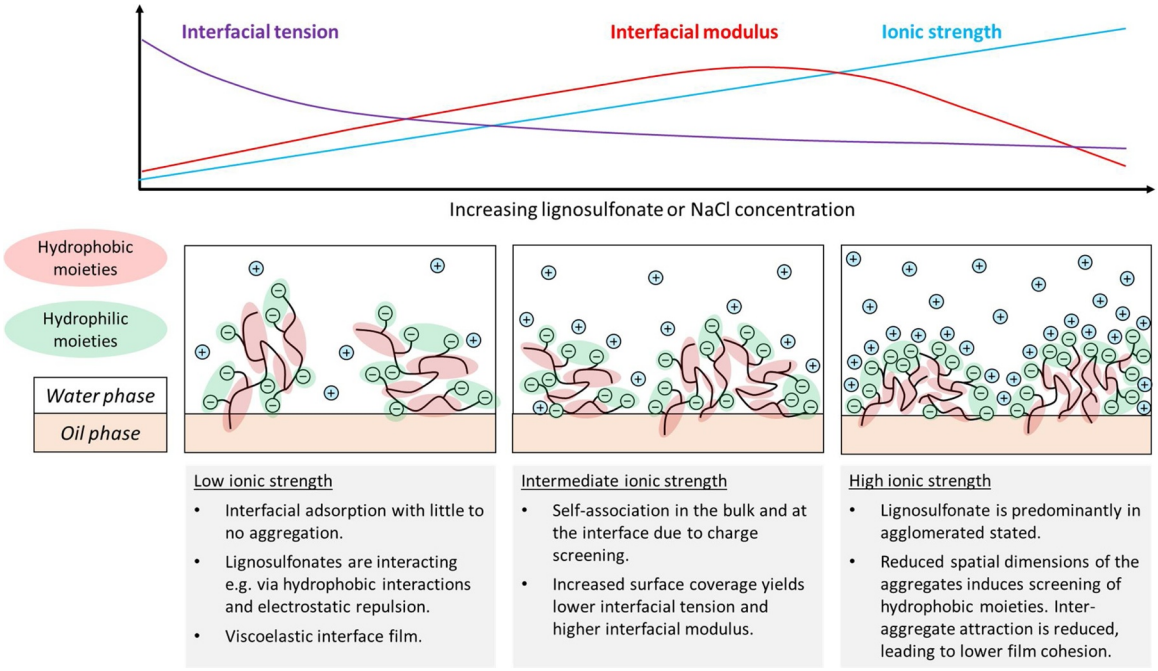

Fig. 16. Schematic of the proposed mechanism for explaining the interfacial tension and modulus trends in dependence of lignosulfonate or NaCl concentration.

compared to sodium ions alone. Lignosulfonate-cation complexation and intermolecular or interaggregate bridging was proposed as the mechanism of action.

Overall, similar trends were observed by the two techniques employed for interfacial rheology. Increasing either lignosulfonate or salt concentration led to first increasing and then decreasing interfacial storage modulus. The emulsion stability was highest at salinities close to the maximum storage modulus. In addition, salting out experiments revealed a concurring of the maximum storage modulus with lignosulfonate agglomerate growth or precipitation. These results agree with the general perception that the stabilization efficiency of a surfactant is usually best, if the surfactant is close to the precipitation limit.

High salinity or high lignosulfonate concentration yielded reduced interfacial film strength. Two mechanisms were proposed to explain this behavior: (1) In case of sodium as the cation, the lignosulfonate molecules or aggregates would contract at high ionic strength, due to screening and reduced dissociation of the anionic groups. This compaction would sterically shield the hydrophobic functional groups, such as aromatic ring structures, which account for attractive interactions between lignosulfonate molecules or aggregates. This loss of cohesion further resulted in a decrease of interfacial modulus. (2) Precipitation occurred in presence of calcium or aluminum cations, which reduced the effective bulk concentration. A lower surface coverage would result in a lower interfacial modulus.

At last, modelling of the interfacial behavior of lignosulfonates was done. Assuming Langmuir adsorption, the diffusion coefficients were determined via the long-time approximation of Ward and Todai. Interfacial adsorption appeared to be affected by lignosulfonate aggregation, as the diffusion coefficient decreased with increasing lignosulfonate concentration. The determined diffusion coefficients were several magnitudes lower than the expected value for single lignosulfonate molecules. This was confirmed by fitting the model by Lucassen and van den Tempel (LvdT) to the interfacial storage and loss modulus. It was hence concluded that the model assumptions were not applicable, and that lignosulfonate adsorption is not diffusion-controlled.

In this article, a detailed investigation of the interfacial behavior of lignosulfonates was presented. We hope that the presented findings can contribute to a better understanding of lignosulfonate behavior at interfaces, and to efficient utilization in technical applications.

CRediT authorship contribution statement

Jost Ruwoldt: Conceptualization, Data curation, Formal analysis, Investigation, Methodology, Validation, Visualization, Writing - original draft, Writing - review & editing. **Sébastien Simon:** Conceptualization, Methodology, Supervision, Validation, Writing - review & editing. **Gisle Øye:** Conceptualization, Funding acquisition, Methodology, Project administration, Supervision, Writing - review & editing.

Declaration of Competing Interest

The authors reported no declarations of interest.

Acknowledgements

This work was carried out as part of the project *Ligno2G: 2nd generation performance chemicals from lignin*, grant number 269570. The authors gratefully acknowledge the financial support from the Norwegian Research Council and Borregaard AS.

References

[1] R.A. Lauten, B.O. Myrvold, S.A. Gundersen, New developments in the commercial utilization of lignosulfonates, Surfactants Renewable Res. (2010) 269–283.
[2] C. Xu, F. Ferdosian, Utilization of lignosulfonate as dispersants or surfactants, in: C. Xu, F. Ferdosian (Eds.), Conversion of Lignin into Bio-Based Chemicals and Materials, Springer-Verlag, Berlin, Heidelberg, 2017, pp. 81–90.
[3] O. Ingruber, M. Kocurek, A. Wong, Pulp and paper manufacture: vol. 4: sulfite science and technology, The Joint Texbook Committee of the Paper Industry (TAPPI/CPPA). cap. VIII, (1985).
[4] H. Sixta, Handbook of Pulp, Wiley-vch, 2006.
[5] B.O. Myrvold, Salting-out and salting-in experiments with lignosulfonates (LSs), Holzforschung 67 (2013) 549–557.
[6] W. Boerjan, J. Ralph, M. Baucher, Lignin biosynthesis, Annu. Rev. Plant Biol. 54 (2003) 519–546.
[7] H.H. Nimz, D. Robert, O. Faix, M. Nemr, Carbon-13 NMR spectra of Lignins, 8. Structural differences between lignins of hardwoods, softwoods, grasses and compression wood, Holzforschung (1981) 16.
[8] G.E. Fredheim, B.E. Christensen, S.M. Braaten, Comparison of molecular weight and molecular weight distributions of softwood and hardwood lignosulfonates, J. Wood

Chem. Technol. 23 (2003) 197–215.
[9] B.O. Myrvold, Differences in solubility parameters and susceptibility to salting-out between softwood and hardwood lignosulfonates, Holzforschung 70 (2016) 1015–1021.
[10] B.O. Myrvold, The Hansen solubility parameters of some lignosulfonates, Int. J. Energy Power Eng. 9 (2015) 261–264.
[11] U. Vainio, R.A. Lauten, R. Serimaa, Small-angle X-ray scattering and rheological characterization of aqueous lignosulfonate solutions, Langmuir 24 (2008) 7735–7743.
[12] U. Vainio, R.A. Lauten, S. Haas, K. Svedström, L.S.I. Veiga, A. Hoell, R. Serimaa, Distribution of counterions around lignosulfonate macromolecules in different polar solvent mixtures, Langmuir 28 (2012) 2465–2475.
[13] M. Yan, D. Yang, Y. Deng, P. Chen, H. Zhou, X. Qiu, Influence of pH on the behavior of lignosulfonate macromolecules in aqueous solution, Colloids Surf. A Physicochem. Eng. Asp. 371 (2010) 50–58.
[14] K.M. Askvik, Complexation of Lignosulfonates With Multivalent Cations and Cationic Surfactants, and the Impact on Emulsion Stability, Department of Chemistry, University of Bergen, Bergen, 2000.
[15] Y. Qian, Y. Deng, X. Qiu, J. Huang, D. Yang, Aggregation of sodium lignosulfonate above a critical temperature, Holzforschung 68 (2014) 641–647.
[16] Q. Tang, M. Zhou, D. Yang, X. Qiu, Effects of pH on aggregation behavior of sodium lignosulfonate (NaLS) in concentrated solutions, J. Polym. Res. 22 (2015) 50.
[17] Y. Deng, Y. Wu, Y. Qian, X. Ouyang, D. Yang, X. Qiu, Adsorption and desorption behaviors of lignosulfonate during the self-assembly of multilayers, BioResources 5 (2010) 1178–1196.
[18] M.A. Zulfikar, D. Wahyuningrum, S. Lestari, Adsorption of lignosulfonate compound from aqueous solution onto chitosan-silica beads, Sep. Sci. Technol. 48 (2013) 1391–1401.
[19] Y.-X. Pang, X.-Q. Qiu, D.-J. Yang, H.-M. Lou, Influence of oxidation, hydroxymethylation and sulfomethylation on the physicochemical properties of calcium lignosulfonate, Colloids Surf. A Physicochem. Eng. Asp. 312 (2008) 154–159.
[20] K.R. Ratinac, O.C. Standard, P.J. Bryant, Lignosulfonate adsorption on and stabilization of lead zirconate titanate in aqueous suspension, J. Colloid Interface Sci. 273 (2004) 442–454.
[21] O. Rojas, J.-L. Salager, Surface activity of bagasse lignin derivatives found in the spent liquor of soda pulping plants, Tappi journal 77 (1994) 169–174.
[22] K.M. Askvik, S. Are Gundersen, J. Sjöblom, J. Merta, P. Stenius, Complexation between lignosulfonates and cationic surfactants and its influence on emulsion and foam stability, Colloids Surf. A Physicochem. Eng. Asp. 159 (1999) 89–101.
[23] D. Rana, G. Neale, V. Hornof, Surface tension of mixed surfactant systems: lignosulfonate and sodium dodecyl sulfate, Colloid Polym. Sci. 280 (2002) 775–778.
[24] X. Qiu, M. Yan, D. Yang, Y. Pang, Y. Deng, Effect of straight-chain alcohols on the physicochemical properties of calcium lignosulfonate, J. Colloid Interface Sci. 338 (2009) 151–155.
[25] V. Hornof, G. Neale, J. Margeson, C. Chiwetelu, Lignosulfonate-based mixed surfactants for low interfacial tension, Cellulose chemistry and technology 18 (1984) 297–303.
[26] B. Li, X.P. Ouyang, Structure and Properties of Lignosulfonate With Different Molecular Weight Isolated by Gel Column Chromatography, Advanced Materials Research, Trans Tech. Publ., 2012, pp. 2024–2030.
[27] S.A. Gundersen, M.-H. Ese, J. Sjöblom, Langmuir surface and interface films of lignosulfonates and Kraft lignins in the presence of electrolyte and asphaltenes: correlation to emulsion stability, Colloids Surf. A Physicochem. Eng. Asp. 182 (2001) 199–218.
[28] Y. Qin, X. Qiu, W. Liang, D. Yang, Investigation of adsorption characteristics of sodium lignosulfonate on the surface of disperse dye using a quartz crystal microbalance with dissipation, Ind. Eng. Chem. Res. 54 (2015) 12313–12319.
[29] Y. Deng, W. Zhang, Y. Wu, H. Yu, X. Qiu, Effect of molecular weight on the adsorption characteristics of lignosulfonates, J. Phys. Chem. B 115 (2011) 14866–14873.
[30] X. Ouyang, Y. Deng, Y. Qian, P. Zhang, X. Qiu, Adsorption characteristics of lignosulfonates in salt-free and salt-added aqueous solutions, Biomacromolecules 12 (2011) 3313–3320.
[31] K.M. Askvik, S. Hetlesæther, J. Sjöblom, P. Stenius, Properties of the lignosulfonate–surfactant complex phase, Colloids Surf. A Physicochem. Eng. Asp. 182 (2001) 175–189.
[32] S.A. Gundersen, J. Sjöblom, High- and low-molecular-weight lignosulfonates and Kraft lignins as oil/water-emulsion stabilizers studied by means of electrical conductivity, Colloid Polym. Sci. 277 (1999) 462–468.
[33] S.A. Gundersen, Ø. Sæther, J. Sjöblom, Salt effects on lignosulfonate and Kraft lignin stabilized O/W-emulsions studied by means of electrical conductivity and video-enhanced microscopy, Colloids Surf. A Physicochem. Eng. Asp. 186 (2001) 141–153.
[34] S.A. Gundersen, Lignosulfonates and Kraft Lignins As Oil-in-water Emulsion Stabilizers, Department of Chemistry, University of Bergen, Bergen, 2000.
[35] B. Biswas, D. Haydon, The coalescence of droplets stabilised by viscoelastic adsorbed films, Kolloid-Zeitschrift und Zeitschrift für Polymere 185 (1962) 31–38.
[36] S.R. Derkach, J. Krägel, R. Miller, Methods of measuring rheological properties of interfacial layers (Experimental methods of 2D rheology), Colloid J. 71 (2009) 1–17.
[37] F. Ravera, G. Loglio, V.I. Kovalchuk, Interfacial dilational rheology by oscillating bubble/drop methods, Curr. Opin. Colloid Interface Sci. 15 (2010) 217–228.
[38] B.S. Murray, Interfacial rheology of food emulsifiers and proteins, Curr. Opin. Colloid Interface Sci. 7 (2002) 426–431.
[39] Y. Fan, S. Simon, J. Sjöblom, Interfacial shear rheology of asphaltenes at oil–water interface and its relation to emulsion stability: influence of concentration, solvent aromaticity and nonionic surfactant, Colloids Surf. A Physicochem. Eng. Asp. 366 (2010) 120–128.
[40] S. Simon, S. Subramanian, B. Gao, J. Sjöblom, Interfacial shear rheology of gels formed at the Oil/Water interface by tetrameric acid and calcium ion: influence of tetrameric acid structure and oil composition, Ind. Eng. Chem. Res. 54 (2015) 8713–8722.
[41] R. Krishnaswamy, S. Majumdar, A.K. Sood, Nonlinear viscoelasticity of sorbitan tristearate monolayers at Liquid/Gas interface, Langmuir 23 (2007) 12951–12958.
[42] H. Brenner, Interfacial Transport Processes and Rheology, Elsevier, 2013.
[43] D. Pradilla, S. Simon, J. Sjöblom, J. Samaniuk, M. Skrzypiec, J. Vermant, Sorption and interfacial rheology study of model asphaltene compounds, Langmuir 32 (2016) 2900–2911.
[44] P. Erni, P. Fischer, E.J. Windhab, V. Kusnezov, H. Stettin, J. Läuger, Stress- and strain-controlled measurements of interfacial shear viscosity and viscoelasticity at liquid/liquid and gas/liquid interfaces, Rev. Sci. Instrum. 74 (2003) 4916–4924.
[45] J. Ruwoldt, J. Planque, G. Øye, Lignosulfonate salt tolerance and the effect on emulsion stability, ACS Omega 5 (2020) 15007–15015.
[46] V.J. Verruto, R.K. Le, P.K. Kilpatrick, Adsorption and molecular rearrangement of amphoteric species at oil − Water interfaces, J. Phys. Chem. B 113 (2009) 13788–13799.
[47] E.M. Freer, C.J. Radke, Relaxation of asphaltenes at the toluene/water interface: diffusion exchange and surface rearrangement, J. Adhes. 80 (2004) 481–496.
[48] E.L. Nordgård, S. Simon, J. Sjöblom, Interfacial shear rheology of calcium naphthenate at the Oil/Water interface and the influence of pH, calcium, and in presence of a model monoacid, J. Dispers. Sci. Technol. 33 (2012) 1083–1092.
[49] A.E. Syahputra, J.-S. Tsau, R.B. Grigg, Laboratory evaluation of using lignosulfonate and surfactant mixture in CO2 flooding, SPE/DOE Improved Oil Recovery Symposium, Society of Petroleum Engineers, Tulsa, Oklahoma, 2000.
[50] D.M. Sztukowski, H.W. Yarranton, Rheology of asphaltene − toluene/water interfaces, Langmuir 21 (2005) 11651–11658.
[51] M. Benmekhbi, S. Simon, J. Sjöblom, Dynamic and rheological properties of span 80 at liquid–Liquid interfaces, J. Dispers. Sci. Technol. 35 (2014) 765–776.
[52] R.J. Nap, I. Szleifer, Effect of calcium ions on the interactions between surfaces end-grafted with weak polyelectrolytes, J. Chem. Phys. 149 (2018) 163309.
[53] R. Schweins, K. Huber, Collapse of sodium polyacrylate chains in calcium salt solutions, Eur. Phys. J. E 5 (2001) 117–126.
[54] A. Sommerauer, D.L. Sussman, W. Stumm, The role of complex formation in the flocculation of negatively charged sols with anionic polyelectrolytes, Kolloid-Zeitschrift und Zeitschrift für Polymere 225 (1968) 147–154.
[55] L.E. Nielsen, R. Wall, G. Adams, Coalescence of liquid drops at oil-water interfaces, J. Colloid Sci. 13 (1958) 441–458.
[56] T.F. Tadros, Emulsion Formation and Stability, Wiley, 2013.
[57] J. Eastoe, J.S. Dalton, Dynamic surface tension and adsorption mechanisms of surfactants at the air–water interface, Adv. Colloid Interface Sci. 85 (2000) 103–144.
[58] A.-K. Kontturi, Diffusion coefficients and effective charge numbers of lignosulphonate. Influence of temperature, J. Chem. Soc., Faraday Transac. 1: Phys. Chem. Condensed Phases 84 (1988) 4043–4047.
[59] A.F.H. Ward, L. Tordai, Time-dependence of boundary tensions of solutions I. The role of diffusion in time-effects, J. Chem. Phys. 14 (1946) 453–461.
[60] A. Einstein, Über die von der molekularkinetischen Theorie der Wärme geforderte Bewegung von in ruhenden Flüssigkeiten suspendierten Teilchen, Ann. Phys. 322 (1905) 549–560.
[61] D. Pradilla, S. Simon, J. Sjöblom, Mixed interfaces of asphaltenes and model demulsifiers part I: adsorption and desorption of single components, Colloids Surf. A Physicochem. Eng. Asp. 466 (2015) 45–56.
[62] A.L. Nenningsland, S. Simon, J. Sjöblom, Influence of interfacial rheological properties on stability of asphaltene-stabilized emulsions, J. Dispers. Sci. Technol. 35 (2014) 231–243.
[63] J. Lucassen, M. Van Den Tempel, Dynamic measurements of dilational properties of a liquid interface, Chem. Eng. Sci. 27 (1972) 1283–1291.
[64] B.O. Myrvold, The polyelectrolyte behavior of randomly branched lignosulfonates, Tappi Journal 6 (2007) 10–14.
[65] Y. Deng, X. Feng, D. Yang, C. Yi, X. Qiu, Pi-Pi stacking of the aromatic groups in lignosulfonates, BioResources 7 (2012) (2012) 12.
[66] B.O. Myrvold, A new model for the structure of lignosulphonates: part 1. Behaviour in dilute solutions, Indust. Crops Prod. 27 (2008) 214–219.
[67] Y. Qian, Y. Deng, X. Qiu, H. Lou, Y. Pang, Slow relaxation mode of sodium lignosulfonate in saline solutions, Holzforschung 69 (2015) 17–23.